The 14th IFToMM World Congress, Taipei, Taiwan, October 25-30, 2015
DOI Number: 10.6567/IFToMM.14TH.WC.OS13.095

Use of Hidden Robot Concept for Calibration of an Over-Constrained Mechanism

G. Kiper[1] M. İ. C. Dede[2] E. Uzunoğlu[3] E. Mastar[4]
İzmir Institute of Technology Coşkunöz Metal Form Inc.
İzmir, Turkey Bursa, Turkey

Abstract: *Overconstrained mechanisms prove useful in applications where high stiffness and low weight is required against high amount of forces while keeping high precision. This study issues a planar two degrees-of-freedom overconstrained parallel manipulator for positioning the end-effector with high acceleration values (>5g) with a positioning precision in the order of 30 μm. Since the manufacturing errors were compatible with the end-effector positioning errors, it was required to perform some system identification before the precision and repeatability tests. For the system identification, the end-effector position and motor input values are recorded. However, since the mechanism is overconstrained, the link lengths could not be obtained due to the lack of analytical inverse kinematics solution. In order to cope with this problem, the hidden robot concept is utilized in order to fit a simple kinematic model between the task space and the joint space of the manipulator. Further calibration studies are carried out using the error correction matrix. The test results are presented.*

Keywords: Hidden robot concept, Overconstrained mechanism, Calibration of manipulators

I. Introduction

There is a continuous need of shortening the process completion durations in manufacturing industry. This need result in the search for new approaches to problems, which has been solved by employing the conventional methods. Any modification to the conventional methods can only result in relatively smaller effects in the betterment of the process completion duration.

It has been a common practice in the manufacturing industry, for planar operations, to use so called x-y tables that have translational two degrees-of-freedom (DoF) that are perpendicular to each other. These operations can be laser or conventional cutting/welding processes. In these operations when the tool dimensions get larger in terms of inertial properties and the workspace is increased, the dimensions of the x-y table increase respectively in mass and inertia. As a result of this, the dynamic characteristics of the total system are affected in a negative way in terms of achievable maximum accelerations. Lower acceleration degrades the mechanism's performance in a more observable fashion when the workpiece has smaller and shaper curved contours to be tracked.

Employment of more powerful actuation systems can be seen as valid modification to the conventional systems. However, this would result in higher magnitude residual vibrations which would call for more rigid structures for the machine and will result in an increase of the inertial properties.

In this work, the problem is redefined as a kinematically redundant system problem by integrating a micro system to the macro system which was previously called as the x-y table. The concept of micro-macro mechanisms is not new. There have been numerous studies in order to incorporate the advantages of both systems in terms of workspace, precision and dynamics [1, 2].

In manufacturing systems, unless the tool is changed, there is a limitation for the maximum process speed. What really limits the performance of the machine in terms of process completion duration is the time spent to reach the maximum speed and come to a full stop. The redundancy concept developed in this work aims at maximizing the acceleration performance of the overall system. Therefore, by incorporating a micro system with smaller inertial properties and higher acceleration performance, the acceleration performance of the overall system is increased. In this setting, macro system is responsible for moving the micro system over the whole workspace. Similar studies on this concept have been carried out and commercial systems have been produced [3, 4, 5].

Our objective in this work was to design and construct a planar manufacturing system that has 1.5 m × 3.0 m workspace, positioning precision of ±30 μm/m, repeatability of ±15 μm/m and highest acceleration of 5 g. The macro mechanism is selected as a conventional x-y table with a cantilever bridge that carries the micro mechanism. The micro mechanism, after much iteration that is explained in [6], is selected as a modified 5-bar mechanism. The mechanism is modified in order to carry a standard tool, use standard servomotors conveniently and maintain the symmetry for improved control quality. As a result, the micro mechanism is designed as an overconstrained 6-bar mechanism. The details of the mechanism are explained in the next section.

In the control scheme of the overall system, the global trajectory designed for the tip point of the tool is divided in to the two systems. Among the numerous algorithms we devised, one of them was presented in [7]. However, independent of which algorithm is used, the trajectory of the micro mechanism is designed in its task space. In order to control the micro mechanism, this task space trajectory has to be translated into its joint space through inverse kinematics. Having an overconstrained mechanism makes the analytical solution for inverse kinematics impossible.

The obvious choice in such a scenario is to use numerical methods for the calculations of inverse kinematics. However, due to the higher dynamics of the applications, the sampling frequency is fairly large for mechanical systems at 2 kHz, which limits the calculations load for real-time operation. In order to devise a solution

[1] gokhankiper@iyte.edu.tr
[2] candede@iyte.edu.tr
[3] emreuzunoglu@iyte.edu.tr
[4] emastar@coskunoz.com.tr

for this problem, a simplified version of the micro mechanism representing its motion and having an analytical inverse kinematics solution is considered based on a number of constraints. This approach was called the hidden robot concept for the first time in [8, 9]. The procedure of the hidden robot concept application for our work is described after the section defining the micro-mechanism.

The overconstrained mechanisms increasing the stiffness of the system also form higher internal stresses. These stress values are not consistent within the workspace of the mechanism, which results in changing link lengths throughout the workspace. Together with the joint clearances this fact makes the calibration process of the mechanism a nontrivial one. The last section of this paper is on the work carried out for the calibration of the overall system again by making use of the hidden robot concept.

II. Description of the Mechanism

In our application, the first mechanism designed for positioning an end-effector in plane was the 5-bar mechanism A_0ACB shown in Fig. 1a. The mechanism is actuated at its fixed revolute joints. The two fixed joint axes are selected to be concurrent and the link lengths are selected to be identical (a = b = c = d) due to the workspace and balancing requirements [7]. Although this 5-bar mechanism can position the end-effector point in its planar workspace, the orientation of the end-effector is not controlled and this results in uncontrolled dynamic effects. Also, when the end-effector object size is comparable with the link lengths, it is not possible to locate the end-effector inside joint C. As a solution to these problems, the mechanism is modified as a 6-bar mechanism A_0ADCEB to obtain a finite moving platform length |DE| (Fig. 1b). In order to keep the end-effector orientation constant, two sets of parallelogram loops are added on the two sides of the arms of the parallel mechanism. Actually, just a pair of parallelogram loops on one side is sufficient to keep the end-effector orientation, but an extra pair of loops is added to keep the symmetry and also overconstrain the mechanism. The positive side of having an overconstrained mechanism is that the stiffness of the mechanism increased and the repeatability is enhanced. The actuators are located at joints A_0 and B_0.

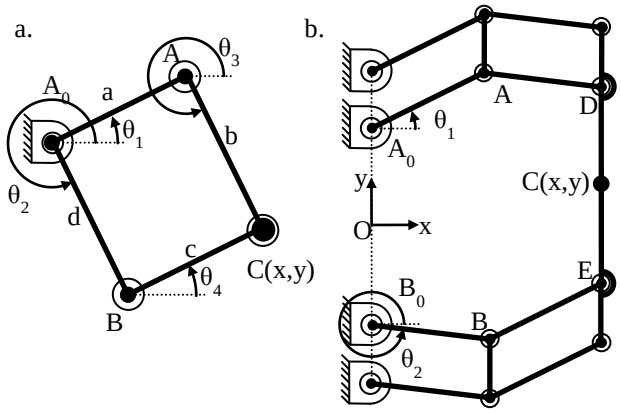

Fig. 1. a. 5-bar mechanism, b. 6-bar mechanism

The two mechanisms shown in Fig. 1 are kinematically equivalent as far as the position of end-effector-point C is concerned. Hence, the simpler kinematic structure in Fig. 1a can be used as the model of the actual mechanism which has the structure in Fig. 1b. Up to this point, theoretically everything is fine. However in practice, the theoretical model does not match with the actual mechanism due to manufacturing tolerance faults, joint clearances and link flexibilities. The joint clearance and link flexibility problem is partly dealt with the overconstrained structure of the mechanism, however the manufacturing faults need to be determined and the model of the mechanism is to be modified accordingly.

It is possible to take measurements on the manufactured assembly in order to modify the model, however in case of an overconstrained system these measurements do not fit to the simpler model. Therefore it is necessary to collect data from the inputs and end-effector point, and then estimate the model parameters from the input/output relationship. The next section presents the methods for model estimation and calibration.

III. Hidden Robot Kinematics

Recently the "hidden robot concept" was proposed for high speed and high precision robotic applications [8, 9]. The hidden robot concept involves the use of a virtual model with simpler kinematic structure in the control algorithm rather than using the rather complicated kinematic structure of the actual robot. This concept was originally developed for the control of a robot for which the end-effector cannot be directly observed [8, 9]. In this study, for the first time, the hidden robot concept is used for the control of an overconstrained mechanism.

For the overconstrained mechanism shown in Fig 1.b there is no analytical inverse kinematics solution when the link lengths are kept arbitrary subject to the condition that the parallelogram loops remain in parallelogram proportions. Therefore use of a simpler (hidden) model (Fig. 1a) for the inverse kinematics proves useful in control and calibration of the mechanism.

For given measured motor and end-effector location data, the model estimation problem is a path generation synthesis problem. We present two different path generation solutions and then explain how the solution is applied for the calibration.

A. Polynomial Approximation

In polynomial approximation synthesis, the link lengths of the mechanism are determined so that the function/path/motion of the end-effector is exactly satisfied at certain precision points. Given a set of inputs (θ_{1i}, θ_{2i}) and end-effector locations $C(x_i, y_i)$ for i = 1, …, n, the link lengths a, b, c, d of the 5-bar mechanism are to be determined. The diads A_0AC and A_0BC are dealt separately. For the A_0AC diad:

$$\begin{aligned} &|AC|^2 = (x_i - a\cdot\cos\theta_{1i})^2 + (y_i - a\cdot\sin\theta_{1i})^2 = b^2 \\ &\Rightarrow b^2 - a^2 + 2\cdot a(x_i\cdot\cos\theta_{1i} + y_i\cdot\sin\theta_{1i}) = x_i^2 + y_i^2 \end{aligned} \quad (1)$$

Eq. (1) can be written in polynomial form:

$$\sum_{j=1}^{2} P_j f_j(\mathbf{x}_i) = F(\mathbf{x}_i) \quad (2)$$

where $\mathbf{x}_i$ represents the set precision point parameters (θ_{1i}, x_i, y_i), $P_1 = b^2 - a^2$, $P_2 = a$, $f_1(\mathbf{x}_i) = 1$, $f_2(\mathbf{x}_i) = 2(x_i \cos\theta_{1i} + y_i \sin\theta_1)$ and $F(\mathbf{x}_i) = x_i^2 + y_i^2$. Given $\mathbf{x}_i$ for i = 1, 2 P_1 and P_2 can be solved linearly from Eq. (2). Once P_1 and P_2 are determined, the link lengths a and b are determined as

$$a = P_2 \quad \text{and} \quad b = \sqrt{a^2 + P_1^2} \quad (3)$$

For dyad A_0BC, Eqs. (1)-(3) can be used by interchanging the parameters; a with d, b with c and θ_1 with θ_2.

B. Least Squares Approximation

Unlike the polynomial approximation, in least squares approximation synthesis, it is not required to exactly satisfy the constraint equations as in Eq. (2), but an error δ_i is allowed:

$$\sum_{j=1}^{2} P_j f_j(\mathbf{x}_i) - F(\mathbf{x}_i) = \delta_i \quad (4)$$

Due to this error, $\mathbf{x}_i$ are no longer called precision points, but they are called design points. The advantage of the method is that the number of design points n can be selected as large as required. In least squares approximation synthesis, the aim is to minimize the summation of the squares of the errors:

$$S = \sum_{i=1}^{n} \delta_i^2 = \sum_{i=1}^{n} \left[\sum_{j=1}^{2} P_j f_j(\mathbf{x}_i) - F(\mathbf{x}_i) \right]^2 \quad (5)$$

Minimization is achieved by equating the partial derivatives of S with respect to P_1 and P_2 to zero:

$$\begin{aligned} \frac{1}{2}\frac{\partial S}{\partial P_1} &= \sum_{i=1}^{n} \left[P_1 f_1(\mathbf{x}_i) + P_2 f_2(\mathbf{x}_i) - F(\mathbf{x}_i) \right] f_1(\mathbf{x}_i) = 0 \\ \frac{1}{2}\frac{\partial S}{\partial P_2} &= \sum_{i=1}^{n} \left[P_1 f_1(\mathbf{x}_i) + P_2 f_2(\mathbf{x}_i) - F(\mathbf{x}_i) \right] f_2(\mathbf{x}_i) = 0 \end{aligned} \quad (6)$$

Eqs. (6) are linear in P_1 and P_2, hence P_1 and P_2 can be determined uniquely.

C. Model Estimation from Measured Data

Several (θ_{1i}, θ_{2i}, x_i, y_i), say N many, values are measured from the real system for model estimation. These measurements were performed with an FARO® interferometer. This device has a measuring precision of ±20 μm. The nine set of data measured with the interferometer are given in Table I. These data are used for the model estimations. The locations (x_i, y_i) are selected as the 4 corners, 4 midpoints of the sides and the center of the rectangular workspace of the mechanism. The link lengths are ideally a = b = c = d = 150 mm. As it can be seen from Table I, the first point is taken as reference; hence the desired and measured coordinate values for this point are equal. The maximum absolute positioning error is observed for point 7 and the amount of error is about 1.5 mm, which is way larger than the target precision value of 30 μm.

			Desired		Measured	
i	θ_1 (°)	θ_2 (°)	x_i (mm)	y_i	x_i (mm)	y_i (mm)
1	45	-45	212.132	0	212.132	0
2	60.881	-21.938	212.132	75	212.55	74.95
3	40.622	-8.689	262.132	75	262.32	74.85
4	29.100	-29.100	262.132	0	262.03	0.04
5	368.689	319.378	262.132	-75	261.82	-74.87
6	381.938	299.119	212.132	-75	211.69	-74.96
7	388.630	281.721	162.132	-75	160.65	-75.18
8	57.286	-57.286	162.132	0	162.22	-0.01
9	78.279	-28.630	162.132	75	163.19	75.08

TABLE I. Measured data

However, there were locations in the workspace that the errors are almost equal to zero. The main reason for this is that the internal stresses on the links of the mechanism change with respect to the position of the tool in the workspace. Therefore, the link lengths are continuously varying while the mechanism is moving to different locations of the workspace.

In order to calculate optimum link lengths that would result in a minimum error within the workspace, the link lengths as they appear in the hidden robot kinematics are iterated by means of the procedure explained below. During the iterations, the measurements with the FARO® interferometer are carried out.

When applying the polynomial approximation, only two of N (= 9 in our case) measurement values can be used. For least squares approximation all of the N measurement values can be used, but this is not necessary. In either case the number of measurement values to be used is bounded as $2 \le n \le N$. n many measurement values are used for the synthesis whereas the error at the remaining N – n many measurements are checked. There are $\binom{N}{n} = \frac{N!}{n!(N-n)!}$ many possible choices of n measurements out of N measurements. The maximum value of the N many absolute errors $\left(\sqrt{\delta_x^2 + \delta_y^2}\right)$ between the calculated and desired values is monitored for each selection of n many measurements and the final selection is done for the minimum value of the maximum error.

All computations are performed in Microsoft Excel®. For polynomial approximation, all possible 36 choices of n = 2 precision points among N = 9 are tried out and the minimum error is obtained for design points 1 and 8. The link lengths are found as a = 149.868 mm, b = c = 150.000 mm and d = 149.890 mm. After the link lengths are modified, the maximum error between the calculated and desired coordinates is evaluated as 93μm. Note that this error value is still a calculated

value, not a measure error. When the measurements are repeated with the new link lengths, it is observed that the positioning error is decreased to the level of 700 μm, which is still not acceptable.

For the least squares approximation, 3-to-9 points can be used for the synthesis. All possible combinations are tried and it is found that the minimum value for the maximum absolute error is found as 90 μm with the selection of points 1, 3, 4 and 8. The new link lengths are calculated as a = 149.959 mm, b = 150.013 mm, c = 150.033 mm and d = 150.040 mm.

Besides the maximum absolute error, also the average and RMS errors for the N measurements points are evaluated and compared for the two approximation methods. The measurements and calculations were performed several times. As it is in this example, it is observed that using polynomial or least squares approximation does not quite differ in the result. It is noteworthy to emphasize that we have also tried more complex hidden robots, such as a 5-bar mechanism with offset between the fixed joint axes. The result is interesting that the simplest model with just four link length parameters together with the simplest approximation method gave the best results in measurements.

Unfortunately the modified link lengths just decreased the positioning error from about 1500 μm to about 700 μm. So, further calibration means are employed, as explained in the next section.

IV. Calibration with an Error Correction Matrix

Any type of manufacturing process has its own tolerance characteristics. Since in this work a manufacturing mechanism is developed, the mechanism has its own tolerances due to its mechanic rigidity and control performance. There will always be manufacturing errors on the parts that are produced for the manufacturing mechanism. However, these errors in the manufacturing of the links and the joints can be tolerated by a suitable calibration process and control parameters can be tuned for better performances.

In our work, when the parts of the mechanism are produced, measurements were taken to check whether they are within the set tolerances. The largest error in a manufactured link was in in range of 100 μm. After all the links are manufactured, the mechanism is assembled by integrating the motors, gears, bearings and the tool. After the assembly process, link lengths are re-measured in a CMM measurement unit and found to be different than the original measurements. The main reasons for the change in the link lengths are the flexibility of the links, internal stress on the links due to having an overconstrained mechanism and the joint clearance. It should be noted that the material for links was chosen as Aluminum in order to have higher strength to weight ratios. Nevertheless, the links were still not rigid enough. Also, repeated CMM measurements showed discrepancies, which we think are due to joint clearances and CMM measurement errors. Therefore, the link lengths calculated according to the CMM measurements were not trustworthy and could not be used to modify our kinematic model.

For calibration of high precision positioning machines, the standard methodology is to construct an error matrix throughout the workspace and feed these errors as corrections to the control inputs. This task is quite straightforward for Cartesian machines with prismatic joints only – which is usually the case in the industry. However, when the relationship between the workspace and joint space parameters is nonlinear, the errors measured in the workspace have to be converted to the necessary corrections in the joint space by means of the mechanism kinematics.

Another interferometer from Renishaw Company is used in this process that has ±1 μm of precision. The set-up for the calibration process is presented in Fig. 2. The workspace of the mechanism is divided into 5 mm × 5 mm grids. The errors in between these points are interpolated in the workspace and then translated into the joint space by using inverse kinematics of the hidden robot.

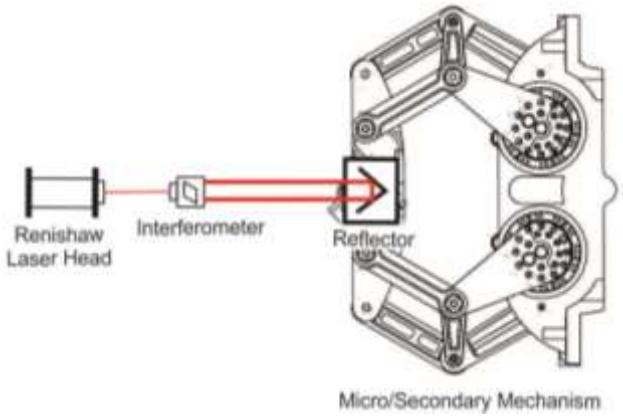

Fig. 2. Calibration process set-up with the Renishaw interferometer

The error correction procedure is as follows: First, i = 1,…,m points along x-axis and j = 1,…,n points along y-axis are selected in the rectangular workspace and hence an m × n many points are selected. In our application, the 100 mm × 150 mm rectangular workspace of the mechanism is divided into 5 mm × 5 mm grids. The positions of the actuated joints corresponding to each grid node are calculated with the updated parameters in inverse kinematics. The control parameters are set to have no steady state error within the workspace. Therefore, there is no error in the controller to contribute in the positioning error of the mechanism. Coordinate measurements are taken at these points and the measured values are subtracted from the desired values to obtain the error matrix $\left[\{\delta_{xi}\}_1^m, \{\delta_{yi}\}_1^m\right]$. The error values for the points besides the selected m × n many points are evaluated using the bilinear interpolation. For the four points $Q_{11}(x_1, y_1)$, $Q_{12}(x_1, y_2)$, $Q_{21}(x_2, y_1)$ and $Q_{22}(x_2, y_2)$ shown in Fig. 2, let the measured x or y coordinate errors be $\delta_{11} = \delta(x_1, y_1)$, $\delta_{12} = \delta(x_1, y_2)$, $\delta_{21} = \delta(x_2, y_1)$, $\delta_{22} = \delta(x_2, y_2)$. Then the error $\delta(x, y)$ at a point P(x, y) in this grid is calculated with bilinear interpolation as

$$\delta(x,y)=\frac{\left\{\begin{array}{l}(x_2-x)(y_2-y)\delta_{11}+(x_2-x)(y-y_1)\delta_{12}\\+(x-x_1)(y_2-y)\delta_{21}+(x-x_1)(y-y_1)\delta_{22}\end{array}\right\}}{(x_2-x_1)(y_2-y_1)} \quad (7)$$

When $x = x_1$ (or $y = y_1$), linear interpolation is performed between Q_{11} and Q_{12} (or Q_{11} and Q_{21}). The error calculation is performed for the x- and y-coordinate error separately. The representation of the bilinear interpolation grid is shown in Fig. 3.

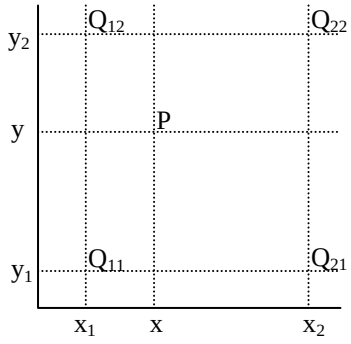

Fig. 3. Bilinear interpolation in a grid

Given the x- and y-coordinate errors (δ_x, δ_y) for a point P(x,y), the input correction values ($\delta_{\theta 1}$, $\delta_{\theta 2}$) are determined using the Jacobian matrix, J, of the manipulator: $[\delta_{\theta 1}, \delta_{\theta 2}]^T = J^{-1}\cdot[\delta_x\ \delta_y\ ]^T$. For the 5-bar mechanism in Fig. 1a.

$$\begin{aligned}\delta_{\theta 1} &= -\frac{\cos\theta_3\cdot\delta_x+\sin\theta_3\cdot\delta_y}{b\cdot\sin(\theta_1-\theta_3)}\ ,\\ \delta_{\theta 2} &= -\frac{\cos\theta_4\cdot\delta_x+\sin\theta_4\cdot\delta_y}{e\cdot\sin(\theta_2-\theta_4)}\end{aligned} \quad (8)$$

In Eq. (8), θ_1 and θ_2 are input angles, hence they are known. θ_3 and θ_4 are found from the kinematic analysis as follows:

$$\begin{aligned}\left|\overrightarrow{CA}\right| &= s=\sqrt{(a\cdot\cos\theta_1-d\cdot\cos\theta_2)^2+(a\cdot\sin\theta_1-d\cdot\sin\theta_2)^2}\\ \measuredangle\overrightarrow{CA} &= \phi=\operatorname{atan2}(a\cdot\cos\theta_1-d\cdot\cos\theta_2,a\cdot\sin\theta_1-d\cdot\sin\theta_2)\\ \theta_3 &= \phi+\pi+\cos^{-1}\left(\frac{b^2+s^2-c^2}{2\cdot b\cdot s}\right),\ \theta_4=\phi-\cos^{-1}\left(\frac{c^2+s^2-b^2}{2\cdot c\cdot s}\right)\end{aligned} \quad (9)$$

Finally, the inputs θ_1 and θ_2 are modified as $\theta_1 - \delta_{\theta 1}$ and $\theta_2 - \delta_{\theta 2}$.

The final calibration procedure is carried out with the complete machine including the macro/primary mechanism and the micro/secondary mechanism. The precision of the complete mechanism is measured to be ±37 μm/m and the repeatability is calculated to be ±26 μm/m. The calculation of these results is compatible with the VDI Standard no VDI/DGQ 3441 - Statistical Testing of the Operational and Positional Accuracy of Machine Tools; Basis.

V. Conclusions

In the work presented in this paper, a micro (secondary) mechanism of a redundant planar manufacturing machine was designed and manufactured. An important feature of this mechanism is that it is an overconstrained mechanism which does not have an analytical inverse kinematics solution. Due to the limitations of the application, numerical solution for the inverse kinematics cannot be used for running the mechanism to accomplish its task.

In order to overrule this limitation, the hidden robot concept is devised for resembling the overconstrained mechanism which has complex kinematics with a mechanism which has simpler kinematics. The kinematics of the hidden robot is used in the control of the redundant machine. It is also used during the calibration process of the mechanism. After using the hidden robot concept in calibration, the precision of the mechanism is improved and the errors decreased by about 40 times. The results of the calibration process are satisfactory in the sense that the precision and repeatability values are comparable with the previously set design criteria for the redundant machine. Finally, this work was a satisfactory example of the hidden robot concept in the control and calibration of complex mechanisms.

Acknowledgements

This study is granted by Republic of Turkey Ministry of Science, Industry and Technology and Coşkunöz Metal Form Inc. (Project code: 01668.STZ.2012-2). The authors thank to Coşkunöz who provided the test equipments.

References

[1] Sharon A. and Hardt D. E. Enhancement of robot accuracy using endpoint feedback and a macro-micro manipulator system. In *American Control Conference*, pp. 1836-1845, San Diego, 1984.

[2] Khatib O. Reduced effective inertia in macro-/mini-manipulator systems, In *The fifth international symposium on Robotics research*, pp. 279-284, 1991.

[3] Leibinger P., Rauser T. and Zeygerman L. Laser Cutting Machine with Multiple Drives. Patent No: US20040178181, 2004.

[4] Masakata M. Punching and Laser Composite Machine, Patent no: JP2006088214, 2006.

[5] Sartorio F. Machine Tool and Manipulator Devise Adapted to be Mounted on Such Machine, Patent no: US20040025761, 2004.

[6] Dede M. İ. C., Gezgin E., Kiper G., Mastar E., Sığırtmaç T. and Uzunoğlu E. Design and analysis of a parallel mechanism for kinematically redundant hybrid planar laser cutting machine. In *16th International Conference on Machine Design and Production*, Vol 2, pp. 810-822, İzmir, 2014.

[7] Uzunoğlu E., Dede M. İ. C., Kiper G., Mastar E. and Sığırtmaç, T. Trajectory planning of redundant planar mechanisms for reducing task completion duration. In *Advances on Theory and Practice of Robots and Manipulators - Proceedings of Romansy 2014 XX CISM-IFToMM Symposium on Theory and Practice of Robots and Manipulators*, Springer, pp. 215-223, 2014.

[8] Briot S. and Martinet P. Minimal representation for the control of Gough-Stewart platforms via leg observation considering a hidden robot model. In *IEEE Int. Conf. on Robotics and Automation*, Karlsruhe, 2013.

[9] Rosenzveig V., Briot S., Martinet P., Ozgur E. and Bouton N. A method for simplifying the analysis of leg-based visual servoing of parallel robots. In *IEEE Int. Conf. on Robotics and Automation*, Hong Kong, 2014.